Materials Research. 2023; 26: e20220444
DOI: https://doi.org/10.1590/1980-5373-MR-2022-0444

Effect of Microalloying on Microstructure and Mechanical Properties of Laser Weld of PHS Steel

***Chunzhi Xia*[a,b]*, *Yinggang Liu*[a], *Xiaoguo Song*[b], *Famin Cong*[a]**

[a]*Jiangsu University of Science and Technology, School of Materials Science and Engineering, Zhenjiang, P. R. China.*
[b]*Harbin Institute of Technology, State Key Laboratory of Advanced Welding and Joining, Harbin, P. R. China.*

Received: October 12, 2022; Revised: : February 19, 2023; Accepted: February 22, 2023

The laser welded joint of 2000MPa cold rolled annealed hot pressed steel (PHS) is easy to break during cold rolling. In this paper, the laser welding method is used to butt weld four kinds of PHS2000 with a thickness of 3.5mm. The four kinds of PHS2000 steel are added with elements of 0% Nb, 0.04% Nb, 0.06% Nb + Cr and 0.08% Nb + Cr. The microstructure of the four kinds of welded joints is compared and analyzed. The mechanical properties of the four kinds of joints are compared through hardness test and tensile test. The results show that after adding 0.04% Nb, residual austenite appears in the weld zone and fully quenched zone, the width of columnar crystal decreases, the average hardness of the weld zone decreases from 595HV to 408HV, and the tensile strength increases from 608MPa to more than 800MPa. For chromium containing steel, the increase of niobium content can reduce the size of columnar crystal in weld zone.

Keywords: *Laser welding, Microalloying, Weld microstructure, Mechanical property.*

1. Introduction

With the rapid development of social economy and the increasing improvement of people's living conditions, private cars have become the most important means of transportation. With the rapid growth of car ownership, people are facing a variety of energy and environmental problems, among which fuel consumption, safety and environmental protection are the top priority[1,2]. The research shows that for every 10.0% reduction in vehicle weight, the fuel consumption can be reduced by about 6.0%[3,4]. In order to give consideration to safety performance, energy conservation and emission reduction, the R & D and application of high-strength and ultra-high-strength automobile steel plates has become an inevitable trend[5]. Microalloying of steel is an important way to improve the properties of traditional structural steel, and niobium has the characteristics of grain refinement, which has been rapidly developed and widely used in microalloying[6,7]. In the process of automobile manufacturing, welding is a common connection method. Compared with the traditional welding method, laser welding has the characteristics of high work efficiency and small heat input, and is widely used by automobile manufacturers[8].

Chen et al.[9] found that the mechanical properties of hot stamping steel containing niobium were better than that of hot stamping steel without niobium, and the uniformity and fineness of microstructure were obviously improved. Lin et al.[10,11] studied the effect of niobium content on the original austenite grain size of 22MnB5 and 38MnB5 hot formed steels. The results showed that after adding niobium, the original austenite grain size reduced from 18.45 μm and 17.0 μm to 10.01 μm and 11.0 μm, respectively. Jo et al.[12] in South Korea also found that the grain size of the microstructure became smaller and grain refinement occurred when niobium alloying was performed in the 1.9 GPa hot stamping steel. Esterl et al.[13] carried out rolling and quenching experiments on steels with different niobium contents, and found that niobium played an important role in delaying recrystallization and could effectively realize grain refinement.

However, for 2000 MPa grade hot rolled steel, the weld is easy to break during cold rolling, which has not been solved. In order to solve this problem, niobium was added into the steel sheet to improve its performance.

2. Materials and Methods

As shown in Table 1, four kinds of cold rolled annealed hot pressed steel (PHS) with different element content were used in this study, all 3.5 mm in thickness. The element contents of these PHS steels were 2# - 0% Nb, 4# - 0.04% Nb, 6# - 0.06% Nb + Cr, 8# - 0.08% Nb + Cr, respectively. The tensile strength of these four PHS steels were 2# 661MPa, 4# 836MPa, 6# 670MPa, 8# 618MPa, respectively.

In this experiment, YLS-6000 fiber laser and ABB welding robot were used to weld the test plates. The main parameters are: output power range 0.6~6kW, laser wavelength 1075nm, the core fiber diameter 200um, the focal length 310nm, and the minimum spot diameter 300um. As shown in Table 2, during welding, the laser power is 5.5kW, the welding speed is 1.8m/min, and the defocus distance is

*e-mail: cz_xia@126.com

Table 1. Main chemical composition of experimental steel plate (w%).

Number	C	Si	Mn	Al	Cr	N	B	Ti	Nb	V
2#	0.33	0.13	1.49	0.06	-	0.0045	0.002	0.03	-	0.16
4#	0.32	0.222	1.54	0.045	-	0.0016	0.0014	0.026	0.04	0.11
6#	0.33	0.25	1.51	0.037	0.33	0.0016	0.0021	0.031	0.062	0.095
8#	0.33	0.24	1.51	0.034	0.33	0.0020	0.0016	0.031	0.083	0.099

Table 2. Laser welding parameters.

Laser power kw	Welding speed m/min	Heat input KJ/cm	Defocus amount mm	Spot diameter mm
5.5	1.8	1.83	-2	0.3

-2mm. Figure 1 shows the position of welding in the steel production process.

The cross section of the weld was polished and corroded. The macro morphology of the weld was observed by Zeiss Axiovert 200 mat optical microscope, and the microstructure of the weld was observed by Zeiss Merlin Compact field emission scanning electron microscope. The hardness of different areas of the weld was measured by MH-5 microhardness tester with parameters: loading force of 200g, applied force of 10s, pressure holding time of 15s, and spacing between each test point of 200 μm.

As shown in Figure 2, take tensile patterns for welds with different components, and stretch the processed tensile samples with CMT5250 electronic universal testing machine at room temperature at a loading speed of 2 mm/min. observe the fracture through JSM-6408 scanning electron microscope.

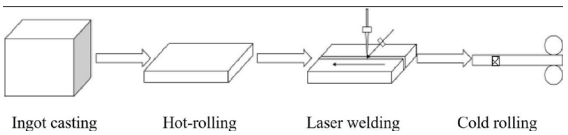

Figure 1. Steel production flow chart.

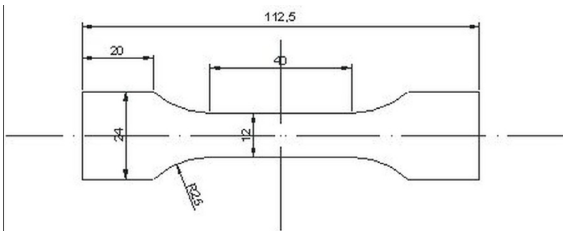

Figure 2. Tensile specimen size.

3. Results and Discussion

3.1. Microstructure analysis of weld zone

Figure 3 shows the microstructure comparison of welding zones with different element contents. 2# (0% Nb) the weld microstructure is lath martensite, which exists in the form of columnar crystal. When the molten pool solidifies, the grain growth direction is perpendicular to the isothermal surface of the liquid metal. Therefore, after the austenite precipitates on the molten pool wall, it grows into columnar crystals along the direction of the maximum temperature gradient and points to the weld center. Because laser welding has the characteristics of high concentration of energy density and extremely fast heating and cooling speed during welding[14], the weld will cool and form martensite in a short time after laser welding.

For 4# (0.04% Nb) sample, the width of columnar crystal in weld zone is decreased from 25.1 μm to 20.1 μm. The grain size becomes smaller, indicating that the addition of 0.04% Nb can effectively reduce the grain size. The microstructure of the weld zone is mainly martensite, but bainite and retained austenite appear. This is because the interaction of trace elements niobium, copper and boron in the steel reduces the bainite transformation temperature, and the bainite transformation can be carried out at a relatively low temperature to form bainite. The microstructure of 6# (0.06% Nb + Cr) weld zone is mainly martensite and bainite. Compared with 4# (0.04% Nb), the content of martensite increases. This is because although the content of niobium increases, the addition of Cr reduces the critical cooling rate of martensite and increases the hardenability of the plate. Therefore, the content of cooling martensite increases under the same conditions after welding. With the increase of Nb content to 0.08%, the width of columnar crystal in weld zone changed from 24.4 μm to 22.6 μm.

3.2. Microstructure analysis of coarse grain zone

Figure 4 shows the microstructure comparison of the coarse-grained zone with different element contents. The coarse-grained zone is a part of the heat affected zone. The peak temperature of the thermal cycle generally exceeds the critical point A_{C3}, and the structure is completely austenitized. When Nb is not added, the microstructure of coarse-grained region is mainly lath martensite with coarse grains, as shown in Figure 4a. After adding 0.04% Nb, there is residual austenite between martensite and the content of martensite decreases, as shown in Figure 4b. Figure 4c and 4d show the coarse-grained regions of 6# and 8# samples respectively. With the addition of Cr, the hardenability of the plate is improved and the martensite content in the coarse-grained zone is increased, which is similar to the change of the microstructure in the weld zone.

3.3. Microhardness analysis

Figure 5 shows the change trend of cross-section hardness of welded joints with different components. It is found that the change trend of hardness of four welded joints is similar.

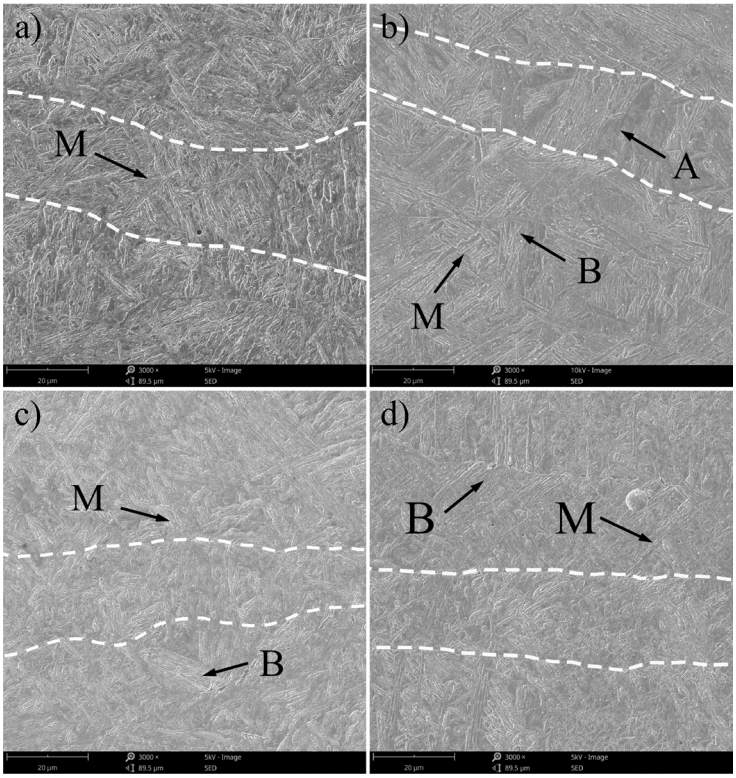

Figure 3. Comparison of microstructure of welding zone with different element content:**(a)** 2#(0%Nb); **(b)** 4#(0.04%Nb); **(c)** 6#(0.06%Nb+Cr); **(d)** 8#(0.08%Nb+Cr).

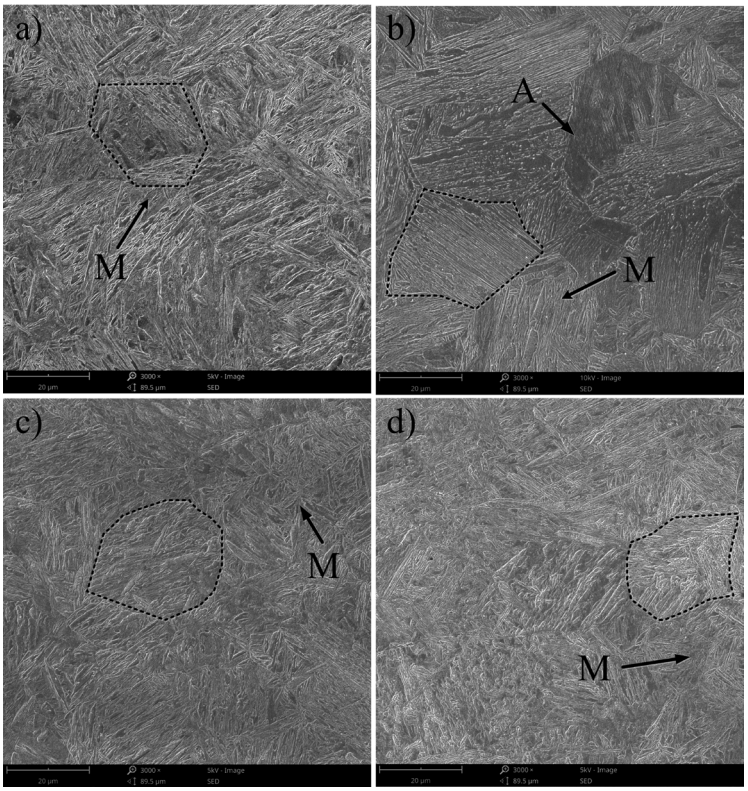

Figure 4. Comparison of microstructure of coarse grain zone with different element content:**(a)** 2#(0%Nb); **(b)** 4#(0.04%Nb); **(c)** 6#(0.06%Nb+Cr); **(d)** 8#(0.08%Nb+Cr).

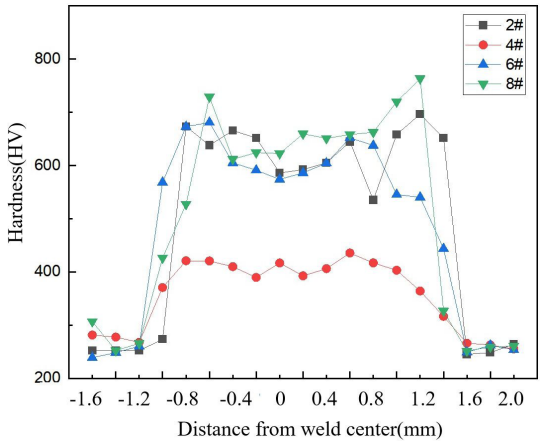

Figure 5. Variation Trend of cross section hardness of welded joints with different components.

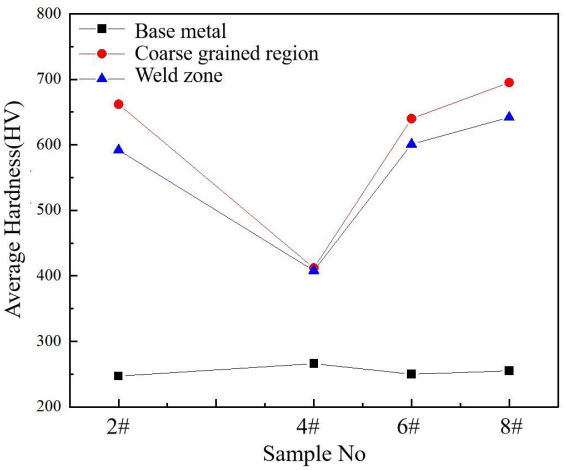

Figure 6. Comparison of average microhardness.

The microhardness curve is approximately M-shaped, the hardness value is symmetrically distributed relative to the weld center, and the hardness of the weld area is significantly higher than that of the base metal. This is because the structure of the weld zone is mainly lath martensite, which belongs to the hardening phase, while the base metal is mainly ferrite and pearlite, and the hardness is low. For 2 # (0% Nb), 6 # (0.06% Nb + Cr) and 8 # (0.08% Nb + Cr), the hardness of the weld coarse-grained zone is significantly higher than that of the weld zone, while for 4 # (0.04% Nb), the hardness of the weld coarse-grained zone is similar to that of the weld zone.

Figure 6 shows the variation trend of average hardness of weld zone, coarse grain zone and base metal with added elements. It is found that the hardness difference of the base metal of the four experimental steels is small, which is about 255HV. 4 # (0.04% Nb) compared with 2 # (0% Nb), the average hardness of the weld area decreased from 595HV to 408HV, and the average hardness of the coarse-grained area decreased from 662HV to 410HV, which is significantly reduced because after adding 0.04% Nb, although the microstructure grains of the weld area became finer, bainite and retained austenite appeared in the microstructure, and the retained austenite in the coarse-grained area increased, resulting in a decreasing trend of the hardness of the two areas. For 6# (0.06% Nb + Cr), the hardness of the weld zone is significantly improved because the martensite content in the weld zone increases after adding Cr to the experimental steel. Although Nb increases at the same time, the effect is not obvious. With the increase of Nb in Cr containing steel from 0.06% to 0.08%, the hardness of weld zone and coarse grain zone increases, because the addition of Nb promotes grain refinement and increases the hardness.

3.4. Tensile strength analysis

Figure 7 shows the macro morphology of the tensile sample. It is found that only 4# (0.04% Nb) tensile sample is broken in the base metal area, about 10 mm away from the weld center. The other three samples are broken in the weld and the heat affected zone adjacent to the weld.

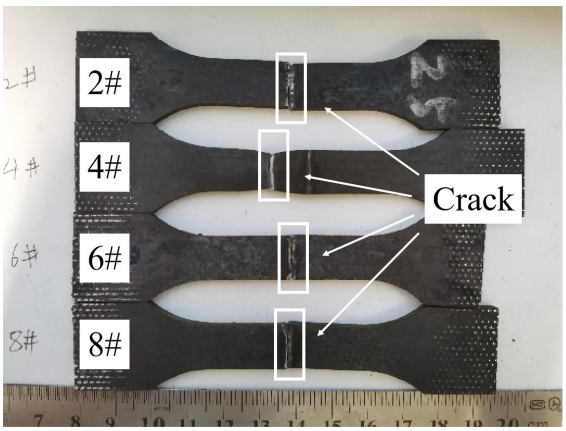

Figure 7. Photo of tensile sample.

Figure 8 shows the tension displacement curves of four welded joints. It is found that except 4# (0.04% Nb) samples, the other three samples belong to brittle fracture. Figure 9 shows the variation trend of tensile strength with element content. 4 # (0.04% Nb) sample is broken in the base metal area, indicating that the tensile property of the weld of this sample is higher than that of the base metal. Compared with 2 # (0% Nb), the tensile strength is increased from 608MPa to more than 800MPa. The broken location of 6 # (0.06% Nb + Cr) sample is the same as that of 2 # (0% Nb), which is broken in the heat affected zone. This is because the coarse-grained zone is mainly martensite with high hardness, which belongs to the hardened phase. With the sharp decline of the hardness value away from the weld zone, the properties of the coarse-grained zone and the base metal zone change obviously, and it is easy to break during tension. With the increase of Nb in Cr containing steel from 0.06% to 0.08%, this gap increases and the tensile strength decreases.

3.5. Fracture morphology analysis

Figure 10 shows the micro morphology of tensile fracture. The fracture morphology of 2# (0% Nb) sample is mainly

dissociated small facets, and many small dimples and longitudinal secondary cracks are also distributed between the dissociated small facets, which is brittle fracture, as shown in Figure 10a. Compared with 2 # (0% Nb), the fracture morphology of 6 # (0.06% Nb + Cr) sample is the same as that of 2 # (0% Nb), but the proportion of dimples increases, there are inclusions in the dimples, and the content of secondary cracks also decreases, which is a mixed ductile brittle fracture, as shown in Figure 10b. With the increase of niobium to 0.08%, the fracture morphology did not change significantly, as shown in Figure 10c.

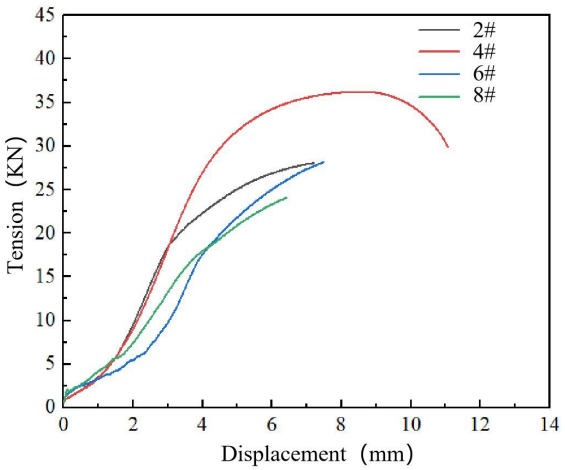

Figure 8. Tension displacement curve.

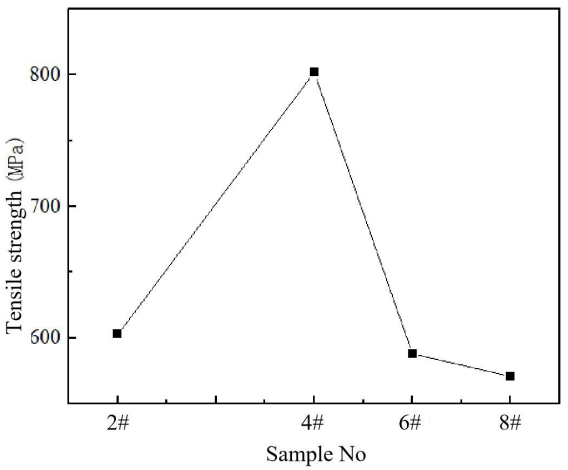

Figure 9. Variation trend of tensile strength.

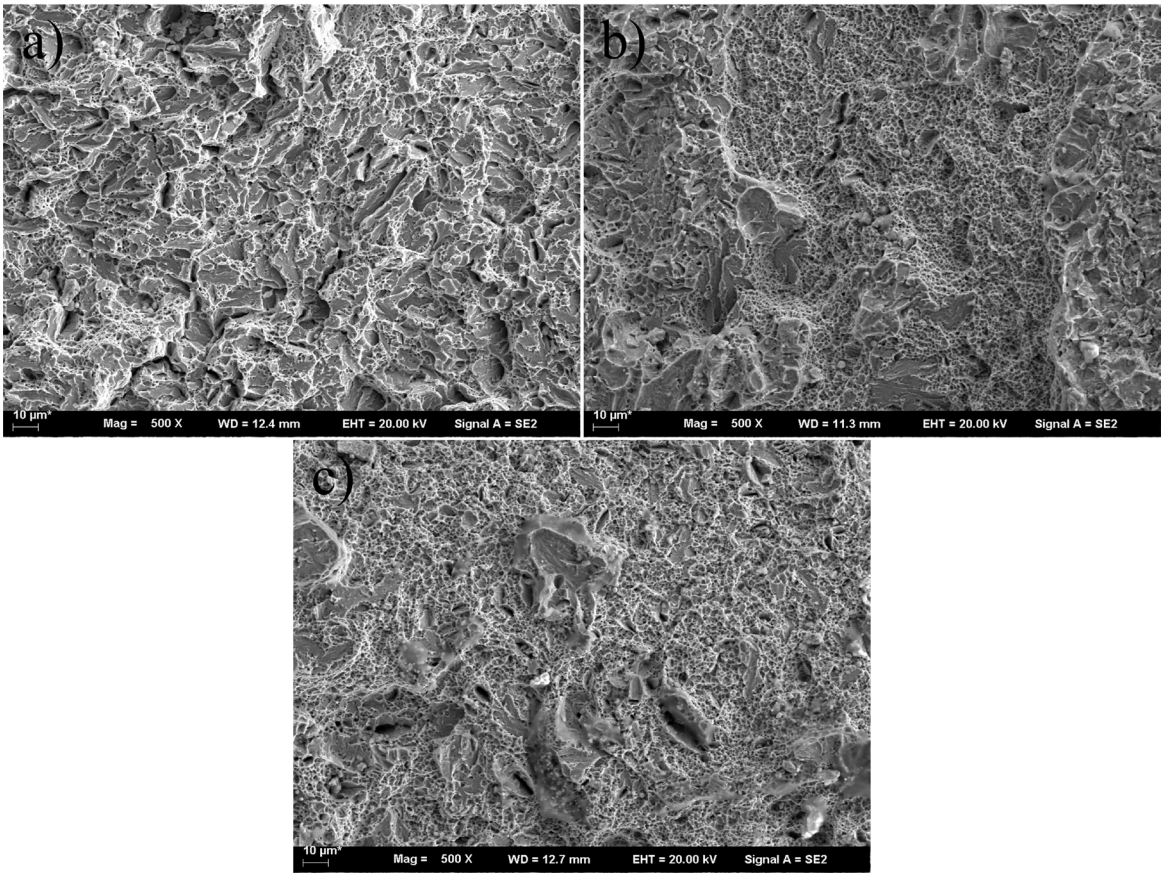

Figure 10. Tensile fracture morphology: **(a)** 2# (0%Nb); **(b)** 6#(0.06%Nb+Cr); **(c)** 8#(0.08%Nb+Cr).

4. Conclusions

(1) Adding 0.04% Nb can reduce the width of columnar crystal in the weld zone, refine the grain, transform the microstructure from martensite to martensite + bainite + retained austenite, and transform the microstructure of coarse grain zone from lath martensite to martensite + retained austenite; The addition of Nb in Cr containing steel increases from 0.06% to 0.08%, the width of columnar crystal in weld zone decreases, and the microstructure is mainly martensite.

(2) The hardness of the welded joint is symmetrically distributed relative to the weld center, the hardness of the coarse-grained zone is the highest, the base metal zone is the lowest, and there is no softening in the heat affected zone. With the addition of 0.04% Nb, the hardness of the welded joint decreased significantly, the hardness of the weld area decreased from 595HV to 408HV, and the gap between the hardness of the coarse-grained area and the weld area decreased.

(3) Adding 0.04% Nb can effectively improve the tensile strength of welded joints. For Cr containing steel, the increase of Nb from 0.06% to 0.08% has no obvious effect on the improvement of weld properties.

5. Acknowledgments

This project was supported by State Key Lab of Advanced Welding and Joining, Harbin Institute of Technology (Grant No. AWJ-21M05) and National Key R&D Program of China (Grant No. 2021YFB3401100).

6. References

1. Mayyas A, Qattawi A, Omar M, Shan D. Design for sustainability in automotive industry: a comprehensive review. Renew Sustain Energy Rev. 2012;16(4):1845-62.
2. Zhao ZZ, Chen WJ, Gao PF, Kang T, Zhao Y, Tang D. Progress and perspective of advanced high strength automotive steel. J Iron Steel Res. 2020;32(12):1059-76.
3. Zhang F, Ruimi A, Wo PC, Field DP. Morphology and distribution of martensite in dual phase (DP980) steel and its relation to the multiscale mechanical behavior. Mater Sci Eng A. 2016;659:93-103.
4. Xie CJ, Yang SL, Liu HB. Microstructure and properties of 7050 ultrahigh-strength aluminum alloy joints by laser welding. Laster Optoelectron Progress. 2018;55(3):357-64.
5. Ashrafi H, Shamanian M, Emadi R, Saeidi N. Correlation of tensile properties and strain hardening behavior with martensite volume fraction in dual-phase steels. Trans Indian Inst Met. 2017;70(6):1575-84.
6. Mohrbacher H, Klinkenberg C. The role of niobium in lightweight vehicle construction. Mater Sci Forum. 2007;537-538:679-86.
7. Erdeniz D, De Luca A, Seidman DN, Dunand DC. Effects of Nb and Ta additions on the strength and coarsening resistance of precipitation-strengthened Al-Zr-Sc-Er-Si alloys. Mater Charact. 2018;141:260-6.
8. Sun Z, Ion JC. Laser welding of dissimilar metal combinations. J Mater Sci. 1995;30(17):4205-14.
9. Chen WJ, Gao PF, Wang S, Lu H, Zhao Z. Effect of vanadium on hydrogen embrittlement susceptibility of high-strength hot-stamped steel. J Iron Steel Res Int. 2021;28(2):211-22.
10. Lin L, Li BS, Zhu G, Kang Y, Liu R. Effect of niobium precipitation behavior on microstructure and hydrogen induced cracking of press hardening steel 22MnB5. Mater Sci Eng A. 2018;721:38-46.
11. Lin L, Li BS, Zhu G, Kang Y, Liu R. Effects of Nb on the microstructure and mechanical properties of 38MnB5 steel. Int J Miner Metall Mater. 2018;25(10):1181-90.
12. Jo MC, Yoo J, Kim S, Kim S, Oh J, Bian J, et al. Effects of Nb and Mo alloying on resistance to hydrogen embrittlement in 1.9 GPa-grade hot-stamping steels. Mater Sci Eng A. 2020;789:139656.
13. Esterl R, Sonnleitner M, Gschöpf B, Schnitzer R. Influence of V and Nb micro-alloying on direct quenched and tempered ultra-high strength steels. Steel Res Int. 2019;90(6):1800640.
14. Riofrío PG, Capela CA, Ferreira JA, Ramalho A. Interactions of the process parameters and mechanical properties of laser butt welds in thin high strength low alloy steel plates. Proc Inst Mech Eng L. 2020;234(5):665-80.